Cancer Chemother Pharmacol (1993) 33: 71–76

Cancer Chemotherapy and Pharmacology

Trofosfamide metabolism in different species – ifosfamide is the predominant metabolite

J. Boos[1], **F. Küpker**[1, 2], **G. Blaschke**[2], **H. Jürgens**[1]

[1] Department of Pediatric Hematology and Oncology, University of Münster, Albert-Schweitzer-Strasse 33, D-48129 Münster, Germany
[2] Institute of Pharmaceutical Chemistry, Hittorfstrasse 58, D-48149 Münster, Germany

Received: 18 December 1992/Accepted: 13 May 1993

Abstract. Trofosfamide (TRO) belongs to the group of oxazaphosphorines and is a congener of cyclophosphamide (CYC) and ifosfamide (IFO). The precondition for the cytotoxic effect of all oxazaphosphorines is their metabolic activation by "ring" oxidation at the hepatic mixed-function oxidase system. In addition, an inactivating metabolic pathway ("side chain" oxidation) is known for CYC and IFO. The metabolic pattern of the substances gains special interest in the discussion of a growing incidence of side effects. Therefore, the in vitro biotransformation of TRO was studied. Liver microsomes were prepared from different species, including the rat, rabbit, and mouse as well as from one human sample. Microsomal proteins were incubated for various periods and concentrations of TRO and its metabolites were analyzed by reversed-phase high-performance liquid chromatography (HPLC). In vitro metabolism resulted in the formation of activated metabolites by hydroxylation at position 4. In addition, side-chain oxidation resulted in the formation of IFO and CYC. IFO was the predominating metabolite of this pathway, with a 5- to 6-fold excess being noted as compared with CYC in rats and mice. The rabbit species showed similar CYC and IFO formation; in the single human sample, only IFO could be detected. In rats, the Michaelis constant (K_m) for biotransformation to IFO was 398 μM, with the maximal volume (V_{max}) being 70.8 nmol 120 min^{-1} mg $protein^{-1}$, the corresponding values for biotransformation to CYC were 348 μM and 13.30 nmol 120 min^{-1} mg $protein^{-1}$. On the basis of its structural similarity and the current knowledge of oxazaphosphorine metabolism, CYC was expected to be the main metabolite of TRO. The predominance of IFO was unexpected, but the observed metabolic profile promises numerous interesting aspects for the clinical use of TRO.

One of the authors (F. K) did most of the work as part of his PhD thesis

Correspondence to: Dr. Joachim Boos, University of Münster, Department of Pediatric Hematology and Oncology, Albert-Schweitzer-Strasse 33, D-48129 Münster, Germany

Introduction

Trofosfamide (TRO) belongs to the group of oxazaphosphorines and is a congener of cyclophosphamide (CYC) and ifosfamide (IFO). Oxazaphosphorines are prodrugs and require metabolic activation at the mixed-function oxidase system of the liver. The activating metabolic reaction is hydroxylation at ring position 4 [6, 9]. The 4-OH metabolite converts to the related aldehyde 4-aldo metabolite, and in a subsequent step, spontaneous elimination of acrolein leads to the alkylating oxazaphosphorine mustard.

Beside this activating metabolic pathway, the catabolic "side-chain oxidation" of the cyclic (at the nitrogen at position 3) and exocyclic (N-position 2) chloroethyl groups has been demonstrated [6, 12, 13]. The different metabolic patterns of CYC and IFO, especially the formation of side-chain metabolites, are currently being intensively discussed in the context of an increasing incidence of renal and central nervous system side effects.

TRO shows the two exocyclic chloroethyl side chains (position 2, like CYC) and, in addition, the side chain at the cyclic nitrogen (position 3, like IFO; see Fig. 1). In contrast to CYC and IFO, information about TRO metabolism is minimal, but side-chain oxidation should be expected to result in CYC and IFO and, therefore, contrary to observations in those drugs, is not a directly inactivating pathway. TRO can be given orally and is well tolerated, according to some clinical reports [2, 7]. The substance might be an alternative to IFO and CYC in outpatient treatment protocols, and the metabolic pattern therefore deserves to be investigated.

Materials and methods

Chemicals

TRO, ISO, CYC, and 5,5-dimethyl-CYC were kindly supplied by Asta Medica (Frankfurt/Main, Germany). Spectrograde solvents such as isopropanol, dichloromethane, acetic acid, and acetonitrile used in extraction or analytical

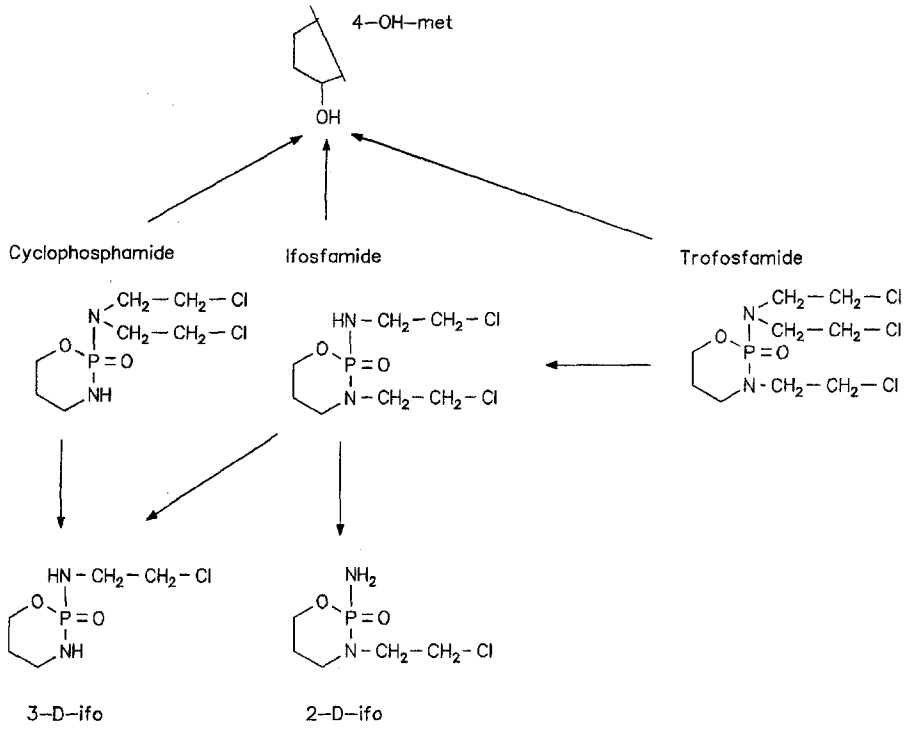

Fig. 1. Structure and metabolism of IFO, CYC, and TRO. 4-OH metabolites (*4-OH-met*) are converted to the tautomere 4-aldo metabolites and achieve antineoplastic activity by spontaneous release of acrolein and formation of oxazaphosphorine mustard. Further oxidation of 4-OH-met/4-aldo-met results in inactive keto and carboxy forms (not shown)

procedures were purchased from Baker (Groß-Gerau, Germany). Reduced nicotinamide adenine dinucleotide phosphate (NADPH), magnesium chloride, and TRIS (hydroxymethyl)aminomethane hydrochloride used in incubation mixtures were purchased from Merck (Darmstadt, Germany). Hydrochloric acid, hydroxylamine hydrochloride, and 3-aminophenol p.a. used in derivatization procedures were purchased from Merck, and acrolein and trans-2-hexenal was obtained from Sigma (Deisenhofen, Germany).

Preparation of enzymes

Male Sprague-Dawley rats (300±50 g), NMRI mice (30±2 g), and female New Zealand white rabbits (2.4 kg ± 350 g) were kept in individual cages and were given free access to commercial food pellets and water ad libitum. Enzymatic activity was not induced by any drug.

After the animals had been exsanguinated by decapitation, the livers were removed, weighed, and washed with buffer solutions. The livers were homogenized in 3 vol. of ice-cold 150 m*M* KCl in 10 m*M* sodium-potassium phosphate buffer (pH 7.4) and centrifuged at 10,000 *g* for 15 min. The postmitochondrial supernatants were centrifuged at 100,000 *g* for 60 min. The microsomal protein content was determined according to Bradford [4] using bovine serum albumin (BSA) as the internal standard. The total cytochrome P_{450} content of microsomal preparations was determined according to Omura and Sato [14].

The single human sample was obtained from a surgical specimen from a 1-month-old newborn hemihepatectomized for a cavernous hemangioma. About 4 g of macroscopically normal liver parenchyma was ice-cooled directly after excision and the enzymes were prepared immediately.

TRO incubation and extraction of the metabolites

After preincubation for 5 min at 37° C, the liver microsome preparation was incubated for specified times at 37° C in a shaking water bath in incubation medium containing NADPH (1 m*M*), magnesium chloride (3.77 m*M*), and TRO at different concentrations. Immediately afterward, the incubation was stopped by placing the incubation tubes on ice. All incubations were done in triplicate.

Assay for determination of side-chain oxidation metabolites

In all, 1490 µl of incubation medium and 100 µl of internal standard solution (87.3 µg 5,5-dimethyl-CYC/ml) were mixed and an aliquot of ice-cold acetonitrile was added to precipitate the protein. After 10 s of vortex mixing, the solution was placed on ice for 10 min. The tubes were centrifuged for 10 min at 4,000 rpm. The supernatant liquid was transferred to clean centrifuge tubes and evaporated to half of the original volume under a stream of nitrogen. The residual liquid was extracted twice with a solution (3 ml) of dichloromethane/isopropanol/acetic acid (85:15:1, by vol.). The extraction medium was then transferred to another tube and evaporated to dryness under a stream of nitrogen. The sample was stored at –20° C until analysis. Then, 200 µl of HPLC eluent was added to the residue, which was vortex-mixed for 20 s and subjected to high-performance liquid chromatographic (HPLC) analysis. 2-Deschloroethyl- and 3-deschloroethyl-IFO were de-

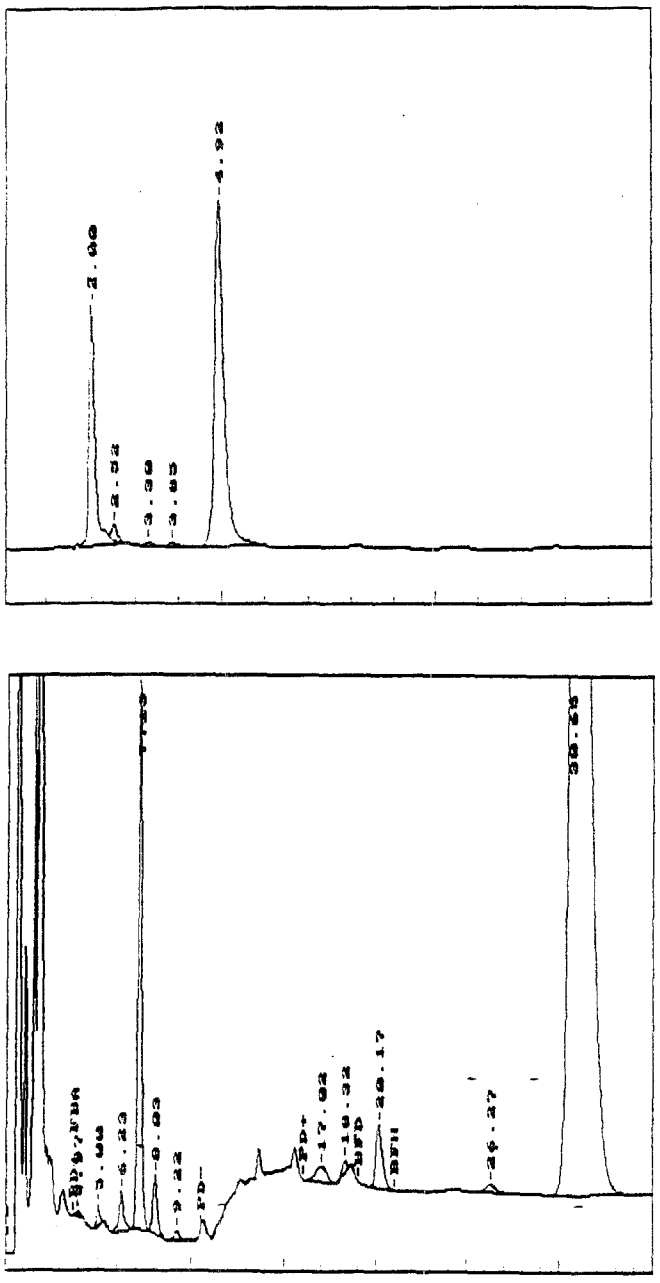

Fig. 2. HPLC chromatograms of an incubation of 1 m*M* TRO with non-induced rat liver microsomes (1 m*M* NADPH, 120 min). The *upper chromatogram* shows 7-OH-quinoline (2.00 min) and internal standard (4.92 min); the *lower chromatogram* shows IFO (7.15 min), CYC (8.03 min), interal standard (20.17 min) and TRO (30.65 min)

termined by capillary gas chromatography as described elsewhere [3].

Instrumentation. The HPLC system consisted of a double piston pump (Pharmacia LKB model 2150), a low-pressure mixer for the eluation gradients, an HPLC controller (Pharmacia LKB model 2252), a variable-wavelength UV detector (Waters model 481), and the integration-system Nelson Analytical Software 4.1. For separation of TRO and its metabolites, a reversed-phase Nucleosil C18 column (5 μm; length, 250 mm; inside diameter, 4 mm; Macherey-Nagel, Düren) and a 30-mm precolumn of the same packing material were used.

HPLC procedure. A 200-μl aliquot of the sample was injected into a 100-μl loop. TRO and its metabolites were eluted from the analytical column by the following gradient. A 35-min step gradient was used to separate TRO and its metabolites and to equilibrate the column. The mobile phases were 25% and 60% acetonitrile in water (v/v). IFO and CYC were eluted using 25% acetonitrile for 8.0 min. The concentration of acetonitrile was then increased to 32% over a 0.5-min interval. After 30 min and TRO elution, the concentration was decreased to 25% over a 0.5-min interval and the column was equilibrated with 25% acetonitrile for 4.5 min before the next sample injection. The eluent was continuously degassed by helium. The flow rate was 1.5 ml/min. The detector was set at 195 nm. Peak areas were used for quantification by the internal-standard method (See Fig. 2).

Calibration. Calibration curves were prepared with 14–570 μ*M* IFO, 12–482 μ*M* CYC, and 58–2331 μ*M* TRO in standard microsomal incubation mixtures and resulted in correlation coefficients of >0.987 for CYC and TRO and >0.999 for IFO. The lower limit of detection was 0.5 μg/ml (1.9 μ*M*, 190 n*M* on the column) for IFO, 0.7 μg/ml (2.7 μ*M*) for CYC, and 0.9 μg/ml (2.8 μ*M*) for TRO.

Recovery. The mean recovery as determined in the microsomal incubation mixtures (protein content, 0.83 mg/ml) was 88.0% ± 5.6% for IFO, 85.3% ± 3.0% for CYC, and 82.2% ± 2.1% for TRO.

Reproducibility. The coefficient of variation according to the peak ratio (compound/internal standard) in standard incubation mixtures for 4 days was 7.8% and 8.3% for IFO (28 and 285 μ*M*, respectively), 9.5% and 6.5% for CYC (28 and 285 μ*M*, respectively), and 6.2% (58 μ*M*) and 5.9% (1,165 μ*M*) for TRO.

Assay for determination of activated metabolites

Incubation samples containing activated metabolites are heated at 100°C under acidic conditions. The released acrolein reacts with 3-aminophenol to form 7-OH-quinoline (7-OH-QU), which can be detected fluorometrically [1].

Incubation medium (100 μl) was transferred into new centrifuge tubes; 100 μl of an internal-standard solution of 1 m*M* trans-2-hexenal and 400 μl of a reaction mixture of 3 *N* hydrochloric acid, 0.5% 3-aminophenol, and 0.6% hydroxylamine hydrochloride were added and the solution was vortexed for 15 s. The reaction was carried out for 6 min at 100°C. The tubes were transferred to ice and 1,000 μl of HPLC-grade water was added. The mixture was then vortexed and centrifuged for 5 min at 4,000 rpm. A 200 μl aliquot of the supernatant was subjected to HPLC analysis.

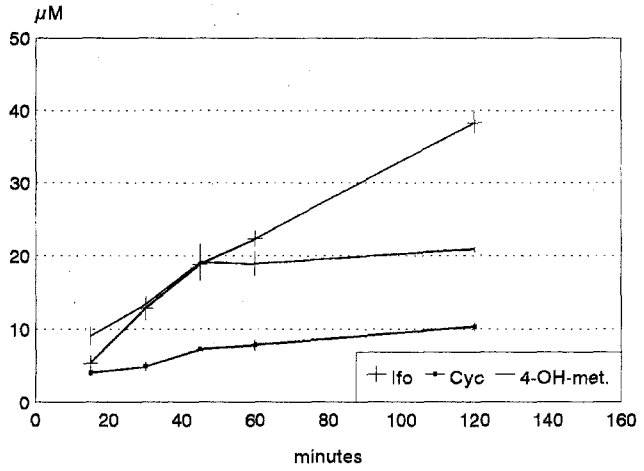

Fig. 3. Concentrations (mean ±SD) of IFO, CYC, and 4-OH metabolites (*4-OH-met.*) versus time of incubation

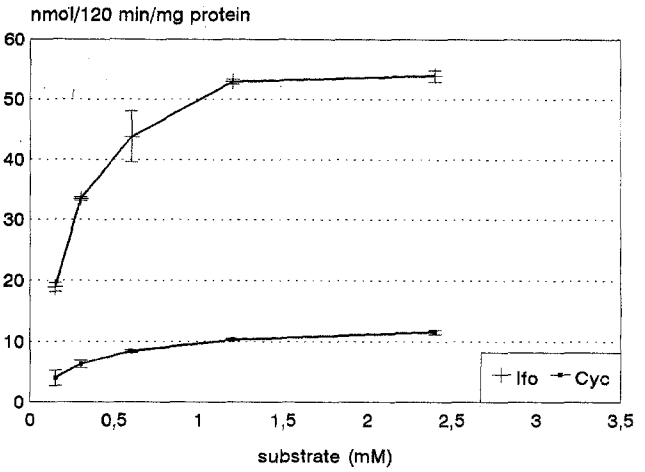

Fig. 4. Concentrations (mean ± SD) of the products IFO and CYC dependent on the concentration of the substrate TRO (120-min incubation, related to 1 mg of protein)

Instrumentation. The HPLC-equipment as prescribed used a fluorescence detector (Shimadzu RF 530). For the separation, a reversed-phase Nucleosil C18 column (5 µm; length, 125 mm; inside diameter, 4 mm; Macherey-Nagel, Düren) and a 30-mm precolumn of the same packing material were used. Peak areas were quantified by the internal-standard method.

HPLC procedure. The mobile phase consisted of acetonitrile/acetic acid/water (15:4:81, by vol.) and was pumped isocratically at a flow rate of 1.0 ml/min. The retention times of the internal standard and 7-OH-QU were 5.1 and 2.0 min, respectively. The excitation wavelength was set at 354 nm and the emission wavelength, at 505 nm (see Fig. 2).

Calibration. The calibration curve (1.5–25 µ*M*) obtained from peak areas gave correlation coefficients of >0.997 with a limit of detection at 0.06 µ*M*.

Reproducibility. The coefficient of variation obtained from derivatization procedures on 5 different days were 12.5% for 3.12 µ*M* acrolein and 8.8% for 25 µ*M* acrolein.

Results

TRO metabolism as a function of incubation time

The experiments were carried out on microsomal preparations (0.83 mg protein/ml) of noninduced rat liver with an excess of TRO (1 m*M*). Over the whole incubation period, significantly higher amounts of IFO were formed. Following 2 h incubation, 10.3 ± 0.5 µ*M* CYC vs 38.3 ± 1.5 µ*M* IFO could be detected. The 4-OH metabolite concentration rose up to 20.9 ± 0.3 µ*M* and the level of TRO decreased to 807.8 ± 0.3 µ*M* (see Fig. 3).

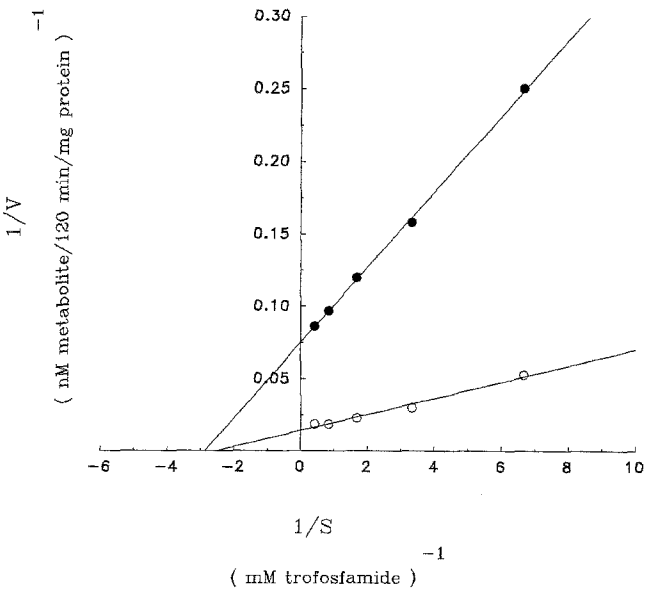

Fig. 5. Lineweaver-Burk plot for TRO metabolism to the metabolites CYC (●) and IFO (○). Linear regression was used to fit the line to the data points, each of which represents the mean value of triplicate determinations

TRO metabolism as a function of substrate concentration

Noninduced rat liver microsomes (0.83 mg protein/ml) were incubated for 120 min at TRO concentrations ranging from 150 µ*M* to 2.4 m*M* (see Fig. 4). IFO formation exceeded CYC formation by a factor of 5 at every concentration tested (0.3 m*M*; 33.4 vs 6.3 nmol 120 min^{-1} mg $protein^{-1}$; 1.2 m*M*; 52.9 vs 11.6 nmol 120 min^{-1} mg $protein^{-1}$). According to the Lineweaver-Burk plot, the maximal volume (V_{max}) was 70.8 nmol 120 min^{-1} mg $protein^{-1}$ for IFO and 13.3 nmol 120 min^{-1} mg $protein^{-1}$ for CYC. The corresponding Michaelis constant (K_m) was 398.0 µ*M* for IFO and 347.8 µ*M* for CYC (see Fig. 5). The subsequent metabolites 2-D- and 3-D-IFO could not be detected in any assay.

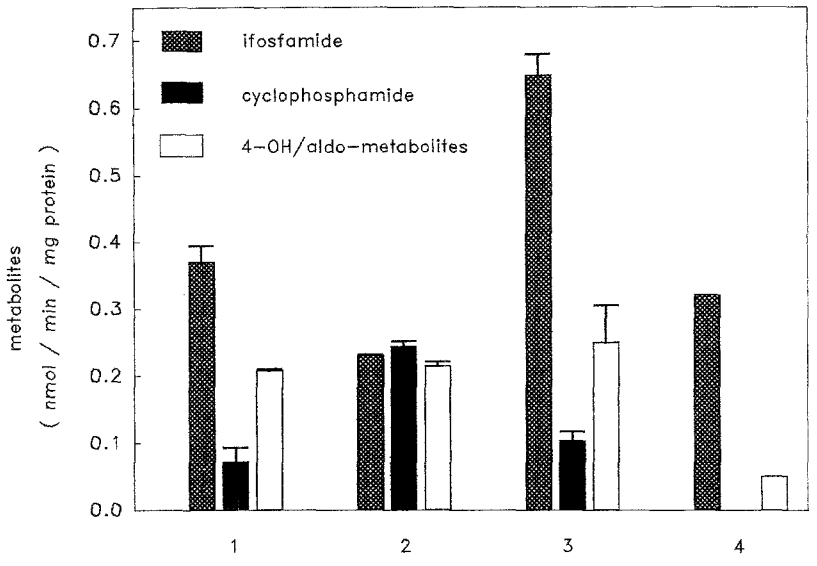

Fig. 6. Formation of IFO, CYC, and 4-OH metabolites in different species. *1*, Rat; *2*, rabbit; *3*, mouse (all determined in triplicate); *4*, human sample (single incubation)

TRO metabolism in different species

Microsomes from rats, rabbits, mice, and one human sample were compared following 120 min incubation with 1 m*M* TRO. The accumulated levels of IFO were 5.1 times higher in rats and 6.2 times higher in mice than the corresponding levels of CYC. In rabbits, the amounts of CYC and IFO were similar. In a single incubation of the human sample, no CYC could be detected (see Fig. 6). The ratio of side-chain-oxidized to ring-oxidized metabolites was comparable in all animal models.

Discussion

In rats, Norpoth et al. [12, 13] observed that TRO metabolites were qualitatively identical to those obtained with CYC and IFO therapy. The results indicated dechloroethylation of TRO, resulting in CYC and IFO, but this was not described further. There was only one different metabolite, assumed to be carboxy-TRO [12, 13]. 4-Hydroxy-TRO, like 4-hydroxy-IFO, shows antitumor activity [9].

In theory, the alkylating activity of TRO could occur in three ways: first, by direct ring oxidation to 4-OH-TRO; second, by dealkylation at position 3, resulting in CYC, and its subsequent oxidation to 4-OH-CYC; and third, via dealkylation at position 2, resulting in IFO, and its subsequent oxidation to 4-OH-IFO. In our assay, however, the determination of 4-OH metabolites via acrolein release could not differentiate between these three activation products.

In CYC and IFO, side-chain oxidation, i.e. oxidative dechloroethylation at position 2 or 3, results in cytostatically inactive metabolites (2-D-IFO, 3-D-IFO = 2-D-CYC). The formation of side-chain oxidation in IFO is more important than that in CYC [13]. In an earlier investigation in children receiving 800–3,000 mg/m^2 IFO i.v., about 14% (range, 9%–29%) of the IFO dose was excreted as 3-D-IFO and about 4% (range, 2%–8%), as 2-D-IFO [5]. This indicates that the metabolic activity of side-chain-oxidizing enzymes in humans is significantly higher at the endocyclic nitrogen than at the exocyclic nitrogen.

Applying this observation to TRO, we expected CYC to be the main side-chain-oxidation metabolite of TRO formed via dechloroethylation at the endocyclic nitrogen (position 3). The outlined results, however, show a clear-cut preference for side-chain oxidation at the exocyclic nitrogen, with IFO being the main side-chain metabolite, which is in contrast to our expectations. In rats and mice, IFO was formed at 5- and 6-fold higher concentrations, and in rabbits the amounts of IFO and CYC were comparable. In the single human sample we found IFO but no CYC. It showed be taken into consideration that the activity of this individual sample was not very high and that CYC may have been formed at the limit of detection. Ifo, however, was the prevailing metabolite in this sample.

Theoretically, a high velocity of further CYC metabolism could account for the predominance of IFO. Therefore, the metabolism of CYC was investigated at three concentrations ranging from 22 to 86 μ*M*, which had been observed as the metabolite concentrations formed in the TRO assay. The decrease of about 20% observed within 2 h of incubation with CYC could not explain the large difference noted between IFO and CYC formation in TRO metabolism. The predominance of IFO, therefore, is primarily based on prevailing IFO formation.

These results are interesting because the oral application of IFO is currently undergoing clinical trials [10, 11] and is limited by the observation of CNS toxicity [15], a side effect that has never been reported for oral TRO. On the one hand, the metabolism of 1 equivalent of TRO may theoretically result in 3 equivalents of chloroacetaldehyde, a metabolite that is purported to cause CNS [8] and renal toxicity. This interrelation, however, has not yet been proven. On the other hand, dechloroethylation of TRO results mainly in IFO and secondly in CYC, both of which products have the capacity to activated by ring oxidation at position 4. In contrast to CYC and IFO, side-chain metabolism of TRO is not necessarily a pathway of inactivation and detoxification.

In the microsomal incubation assay, levels of 2-D- and 3-D-IFO as an expression of subsequent side-chain oxidation of IFO and CYC were under the limit of detection. Theoretically, the side-chain-oxidizing enzymes will primarily be occupied by the metabolism of TRO to IFO and CYC and, therefore, will produce only small amounts of the inactive side-chain products 2-D- and 3-D-IFO. Competition between TRO, CYC, and IFO in side-chain oxidation showed be expected during incubations with an excess of TRO (1 m*M*).

Clinical monitoring of TRO therapy to address this issue is currently in progress. A decrease in the inactivation capacity of side-chain oxidation by the formation of products that are again substrates for the activating pathway, resulting in a metabolic profile with active TRO, IFO, and CYC promises numerous interesting aspects for the clinical use of TRO. While TRO can be applied orally over long periods without producing significant side effects [2, 16], the investigation of TRO metabolism is expected to give new insights into the relationship between drug metabolism and side effects.

References

1. Alacorn RA (1969) Fluorimetric determination of acrolein and related compounds with *m*-aminophenol. Anal Chem 40: 1704–1708
2. Albrecht M, Kleinkauf-Houken A, Trams G, Thomsen K (1984) 5jährige Erfahrungen mit adjuvanter Chemotherapie beim primären Mammakarzinom. Geburtshilfe Frauenheilkd 44: 550–556
3. Blaschke G, Koch U (1986) Untersuchungen zum stereoselektiven Metabolismus von Ifosfamid. Arch Pharm 319: 1052
4. Bradford MM (1976) A rapid and sensitive method for the quantitation of microgram quantities of protein utilizing the principle of protein-dye binding. Anal Biochem 72: 248–254
5. Boos J, Welslau U, Ritter J, Blaschke G, Schellong G (1991) Urinary excretion of the enantiomers of ifosfamide and its inactive metabolites in children. Cancer Chemother Pharmacol 28: 455–460
6. Connors TA, Cox PJ, Farmer PB, Foster AB, Jarman M (1974) Some studies of the active intermediates formed in the microsomal metabolism of cyclophosphamide and isophosphamide. Biochem Pharmacol 23: 115–129
7. Falkson G, Falkson HC (1978) Trofosfamide in the treatment of patients with cancer – a pilot trial. S Afr Med J 53: 886–888
8. Goren MP, Wright RK, Pratt CB, Pell FE (1986) Dechlorethylation of ifosfamide and neurotoxicity. Lancet II: 1219–1220
9. Hohorst HJ, Peter G, Struck RF (1976) Synthesis of 4-hydroperoxy derivatives of ifosfamide and trofosfamide by direct ozonation and preliminary antitumor evaluation in vivo. Cancer Res 36: 2278–2281
10. Kurowski V, Cerny T, Küpfer A, Wagner T (1991) Metabolism and pharmacokinetics of oral and intravenous ifosfamide. J Cancer Res Clin Oncol 117 [Suppl 4]: 148–153
11. Lind MJ, Margison JM, Cerny T, Thatcher N, Wilkinson PM (1989) Comparative pharmacokinetics and alkylating activity of fractionated intravenous and oral ifosfamide in patients with bronchogenic carcinoma. Cancer Res 49: 753–757
12. Norpoth K (1976) Studies on the metabolism of isophosphamide (NSC-109724) in man. Cancer Treat Rep 60: 437–443
13. Norpoth K, Addicks HW, Witting U, Müller G, Raidt H (1975) Quantitative Bestimmung von Cyclophosphamid, Ifosfamid und Trofosfamid sowie ihrer stabilen Metabolite auf der DC-Platte mit 4-Pyridinaldehyd-2-benzothiazolylhydrazon (PHB). Drug Res 25: 1331–1336
14. Omura T, Sato R (1964) The carbon monoxide-binding pigment of liver microsomes. J Biol Chem 239: 2370–2385
15. Wagner T, Drings P (1986) Pharmacokinetics and bioavailability of oral ifosfamide. Drug Res 36: 878–880
16. Wist E, Risberg T (1991) Trofosfamide in non-Hodgkin's lymphoma – a phase II study. Acta Oncol 30: 819–821